BNL-66342-00/03-Rev.

OZONE PRODUCTION IN THE NEW YORK CITY URBAN PLUME

L. I. Kleinman, P. H. Daum, D. G. Imre, J. H. Lee, Y.-N. Lee,
L. J. Nunnermacker, S. R. Springston, J. Weinstein-Lloyd[†], and L. Newman
Atmospheric Sciences Division
Environmental Sciences Department
Brookhaven National Laboratory
Upton, NY 11973-5000

Original Manuscript: March 1999
Revised Manuscript: March 2000

To be published in
Journal of Geophysical Research
(in press)

[†] Chemistry/Physics Department, SUNY/Old Westbury, Old Westbury, NY 11568

This research was performed under the auspices of the U.S. Department of Energy under Contract No. DE-AC02-98CH10886.

Ozone production in the New York City urban plume

Lawrence I. Kleinman, Peter H. Daum, Dan G. Imre, Jai H. Lee,
Yin-Nan Lee, Linda J. Nunnermacker, Stephen R. Springston,
Judith Weinstein-Lloyd, and Leonard Newman

Atmospheric Sciences Division, Brookhaven National Laboratory, Upton, New York

Abstract. In the summer of 1996 the Department of Energy G-1 aircraft was deployed in the New York City metropolitan area as part of the North American Research Strategy for Tropospheric Ozone-Northeast effort to determine the causes of elevated O_3 levels in the northeastern United States. Measurements of O_3, O_3 precursors, and other photochemically active trace gases were made upwind and downwind of New York City with the objective of characterizing the O_3 formation process and its dependence on ambient levels of NO_x and volatile organic compounds (VOCs). Four flights are discussed in detail. On two of these flights, winds were from the W-SW, which is the typical direction for an O_3 episode. On the other two flights, winds were from the NW, which puts a cleaner area upwind of the city. The data presented include plume and background values of O_3, CO, NO_x, and NO_y concentration and VOC reactivity. On the W-SW flow days O_3 reached 110 ppb. According to surface observations the G-1 intercepted the plume close to the region where maximum O_3 occurred. At this point the ratio NO_x/NO_y was 20-30%, indicating an aged plume. Plume values of CO/NO_y agree to within 20% with emission estimates from the core of the New York City metropolitan area. Steady state photochemical calculations were performed using observed or estimated trace gas concentrations as constraints. According to these calculations the local rate of O_3 production $P(O_3)$ in all four plumes is VOC sensitive, sometimes strongly so. The local sensitivity calculations show that a specified fractional decrease in VOC concentration yields a similar magnitude fractional decrease in $P(O_3)$. Imposing a decrease in NO_x, however, causes $P(O_3)$ to increase. The question of primary interest from a regulatory point of view is the sensitivity of O_3 concentration to changes in emissions of NO_x and VOCs. A qualitative argument is given that suggests that the total O_3 formed in the plume, which depends on the entire time evolution of the plume, is also VOC sensitive. Indicator ratios O_3/NO_z and H_2O_2/NO_z mainly support the conclusion that plume O_3 is VOC sensitive.

1. Introduction

High O_3 levels, exceeding the old, but still applicable, federal 1 hour - 120 ppb standard, are experienced in and around the major metropolitan centers of the northeastern United States. In many years, the highest O_3 levels in the northeastern United States occur downwind of the New York City metropolitan area. This region has the dual problem of being a pollutant recipient when winds are from source regions located to the west or southwest and also being a pollutant generator because of its very high population, auto usage, and industrial activity [*National Research Council*, 1991, pp. 98-105; *Ryan et al.*, 1998; *Zhang et al.*, 1998].

The purpose of the North American Research Strategy for Tropospheric Ozone-Northeast (NARSTO-NE) program is to determine the cause of, and control measures for, elevated O_3 in the northeastern United States. To this end, field programs involving aircraft observations and enhanced surface chemical and meteorological measurements were conducted during the summers of 1995 and 1996. This is the first time since the 1980 Northwest Regional Oxidant Study (NEROS) program (centered in the Baltimore-Washington, D. C. area) that the northeast corridor has been the subject of an extensive field campaign aimed at characterizing the three-dimensional (3-D) distribution of O_3 and its precursors. Among the outputs of the NARSTO-NE field intensive is a data set being used for model verification [*Lurmann et al.*, 1997] and for characterizing the interactions between transport and photochemistry [*Blumenthal et al.*, 1997], in particular, the role of high O_3 concentrations in the nighttime residual layer contributing to the next day's O_3 maximum [*Berkowitz et al.*, 1998; *Ryan et al.*, 1998; *Zhang et al.*, 1998].

As part of the overall NARSTO-NE effort, Brookhaven National Laboratory (BNL) along with collaborators from Argonne National Laboratory (ANL), Battelle Memorial Institute (BMI), Environmental Measurements Laboratory (EML), Pacific Northwest National Laboratory (PNNL), and State University of New York (SUNY) Old Westbury conducted the New York City urban plume experiment in the summer of 1996. Measurements were made upwind and downwind of New York City using the Department of Energy (DOE) G-1 aircraft. One focus of these measurements, which is the topic of this study, is to examine the process of O_3 production and its dependence on ambient levels of the O_3 precursors, NO_x and volatile organic compounds (VOCs).

Ozone control is accomplished by reducing emissions of either NO_x or VOCs or both. The optimum strategy varies from place to place in response to such factors as the absolute and relative emission rates of VOCs and NO_x and the contribution of natural sources to the ambient mix of VOCs [*National Research Council*, 1991; *Chameides and Cowling*, 1995; *Sillman*, 1999]. Several qualitative generalizations are possible. In regions where VOC reactivity is dominated by natural emission sources (i.e., isoprene and terpenes from trees), NO_x control can be the only option [*Chameides et al.*, 1988; *Roselle et al.*, 1991]. For regions where anthropogenic sources of VOCs dominate, NO_x control is most effective when emission rates are relatively low; VOC controls become

increasingly effective in high-emission-rate regions [*Sillman*, 1993, 1999].

Urban and regional photochemical grid model calculations that have been used to explore control strategies for O_3 in the northeastern United States [*Rao and Sistla*, 1993; *Roselle et al.*, 1991; *National Research Council*, 1991, pp. 362-375; *Roselle and Schere*, 1995; *Sistla et al.*, 1996] largely confirm these qualitative generalizations. A common finding is that O_3 in the New York City metropolitan area, especially during high-O_3 events and close to the city, is more sensitive to VOC reductions than to NO_x reductions. In this respect, New York City resembles Los Angeles more than it does smaller cities such as Atlanta, Georgia, and Nashville, Tennessee, which have been the subjects of recent field campaigns [*Sillman et al.*, 1997; *Meagher et al.*, 1998, and reference therein].

The problem of formulating an emission control strategy to reduce O_3 levels in the New York City metropolitan area and its downwind region of influence is made complicated by the fact that this region is exposed to pollutants from a variety of discrete source regions as well as a high background. Background O_3, for example, is likely to have a different NO_x and VOC sensitivity than O_3 formed within the New York City metropolitan area plume. In this article we will concern ourselves with O_3 formed downwind of the New York City metropolitan area, recognizing that its properties are dependent upon the background in which it is embedded.

We start with an overview of the New York City experiment, including a description of flights, instruments, and the geographic location of emission sources. Detailed information, including surface O_3 monitoring data, is provided for four case study days in which the G-1 aircraft intercepted the New York City urban plume. On two of these days, wind flow was from the W-SW. On the other two days, wind flow was from the NW. As expected from the geographic distribution of emission sources, west to SW flow conditions are associated with high O_3 (above 100 ppb) while the NW days are much cleaner. Although O_3 concentrations remained below the 120 ppb-1 hour standard, the surface O_3 patterns for W-SW flow are similar to those observed in more severe episodes. Conditions in the plumes are characterized by presenting the concentrations of O_3, CO, NO_x, and NO_y (sum of NO_x and its oxidation products, NO_z; i.e., $NO_y = NO_x + NO_z$), the reactivities of VOC components (broadly defined here to include CO), and the ratios CO/NO_y, NO_x/NO_y, O_3/NO_z, and H_2O_2/NO_z. Comparisons are made with upwind measurements and with the spatially adjacent nonplume air.

Photochemical calculations using observed concentrations of stable species as constraints were performed to determine the rate of O_3 production and its sensitivity to changes in the concentrations of O_3 precursors. The quantities obtained by this type of calculation are local; they relate to the instantaneous state of an air parcel at the time and place where measurements are made [*Kleinman et al.*, 1997; *Kleinman*, 2000; *Daum et al.*, 2000]. We show in this article how this local information is relevant to the nonlocal question of what happens when emissions are changed at some upwind location. As the plume interceptions on the W-SW flow days are close to the time and place where maximum O_3 levels were observed by the surface monitoring network, conclusions reached about NO_x and VOC sensitivity are relevant to the policy issue of how best to control peak O_3 levels.

2. Experiment

The New York City metropolitan area is a high-population and high-emission-rate region. It is located in the northeast corridor, which contains the metropolitan areas of Washington, D. C., Baltimore, Maryland, Philadelphia, Pennsylvania, New York City, and Boston, Massachusetts. Figure 1 is a map of this region showing the places that are referred to in this article. The spatial area of the experiment is indicated by a composite ground track from 13 flights of the DOE G-1 aircraft. More detailed plots are given as we present results (see also, *Roberts et al.* [1996a] for a complete set of ground track plots). All times referred to here are local standard time (LST).

Other elements of the NARSTO-NE program are described in a series of reports from the Electric Power Research Institute (EPRI) and Sonoma Technology, Inc. [*Roberts et al.*, 1996a, b; *Lehrman et al.*, 1997; *Ray et al.*, 1997]. Surface O_3 observations summarized by *Roberts et al.* [1996a] indicate that 1996 was a relatively clean year with about half the O_3 exceedances observed in 1995.

2.1. Flights

Flight patterns directed at following the formation of O_3 in the New York City urban plume were designed to include mid-boundary layer altitude traverses upwind and downwind of the city. It was originally planned that there would be several traverses located at distances ranging from ~20 to 120 km from the urban center. However, air traffic control considerations required that the close-in flight segments be curtailed. Consequently, most of the urban plume flights include only a single downwind crossing. Traverses were done at a fixed altitude, usually between 300 and 700 m, which at the time of the urban plume encounters was within the mixed layer. Flights typically included a vertical profile which serves to identify the top of the mixed layer.

2.2. Instruments

The DOE G-1 aircraft was used to measure the concentrations of trace gas species involved in the photochemical reactions that produce O_3. Measurements included O_3, NO, NO_2, NO_y, peroxyacetylnitrate (PAN) (instrumentation and analysis by BMI), CO, speciated VOCs (canister samples analyzed at York University and ANL), HCHO, H_2O_2, organic peroxides, SO_2, and radon (instrumentation and analysis by EML). Most of these instruments have been previously used and are described in papers reporting results from other field campaigns (see *Nunnermacker et al.* [1998] for O_3, NO, NO_2, NO_y, CO, and SO_2, *Lee et al.* [1996] for HCHO, *Weinstein-Lloyd et al.* [1996] for peroxides; and *Kleinman et al.* [1996] for VOCs).

Data from the continuous trace gas instruments (O_3, NO, NO_2, NO_y, SO_2, CO, and peroxides) were recorded at 1 Hz and averaged over 10 s intervals prior to analysis. Response times for O_3, NO, NO_2, NO_y, and SO_2 were 10s or less, CO had a response time of 30 s, and peroxides had a response time of approximately 1 min. HCHO, PAN, Rn, and VOCs were measured from discrete samples. HCHO samples were collected over a 3 min interval and repeated every 3 mins. PAN measurements were from 30 s long samples at a frequency of once every 7 mins. Between 5 and 20 VOC canisters were filled on each flight. Samples were taken

upwind and downwind of New York City. Exact locations were determined in-flight on the basis of a near-real-time assessment of pollutant conditions. Canisters took 30 s to fill. In addition to the trace gas chemical instruments the G-1 was equipped to measure the size distribution of accumulation mode aerosol particles, temperature, dew point, short-wave solar intensity, and aircraft position.

3. Emissions

Plates 1a and 1b show emission rates for NO_x and CO, respectively, for the region extending from Washington, D. C. to Boston, according to the 1990 National Acid Precipitation Assessment Program inventory [*U. S. Environmental Protection Agency* (EPA), 1993]. Although the entire northeast corridor is a high-emission-rate region, we see from these figures that the New York City metropolitan area stands out as having the highest emission rates. A similar picture is obtained if we look at total anthropogenic VOC emissions or any of its components. Throughout this article we will refer to the source region for the observed plumes as the New York City metropolitan area (or sometimes New York City, for short). Although there is a formal geopolitical definition of a metropolitan area, we will instead be using this designation to mean the high-emission-rate region centered on New York City. This region includes the city proper as well as nearby adjacent areas in New Jersey, Long Island, and Westchester County (to the north). To aid in visualizing this region, three boxes have been drawn on Plates 1a and 1b that are more or less centered on the city proper. The outer box is meant to depict an area with high regional emissions. The inner box includes the highest emission rate areas of New York City; it occupies 8% of the area of the regional box, but contains 47% and 39% of the total regional emissions of NO_x and CO, respectively. The middle box follows most closely our definition of the New York City metropolitan area; it occupies 18% of the area of the regional box but contains 61 and 60% of the total regional emissions of NO_x and CO, respectively. The intent of this particular definition is not to define in detail a source region but rather to show that there is a relatively compact region around New York City, that by virtue of its size and emission density must be responsible for large NO_x and CO plumes observed downwind of the city.

Our expectation based upon these emission maps is that there should be a pronounced and easily identifiable pollutant plume extending downwind from New York City. This was observed some of the time (in particular, for the cases considered in this paper), but on other occasions the plume was diffuse and hard to identify either because it had spread out or it was merged into a high regional background. This limited the number of cases available for analysis.

Under SW flow the region upwind of New York City contains significant emission source, and it is expected that the inflow to New York City will be relatively polluted. Under NW flow conditions, relatively clean air is imported into the city.

4. Photochemical Model

Ozone production rates and their sensitivity to ambient levels of NO_x and VOCs were calculated using a steady state photochemical model constrained with the trace gas concentrations measured on the G-1. The model is zero-dimensional and yields the concentrations of free radicals and NO_2, at a particular point in time and space, that are in rapid equilibrium with the observed (or estimated) mix of longer-lived compounds. We also obtain the formation rate for O_3 and its sensitivity to changes in ambient NO_x and VOC concentration.

As the steady state calculations have been described in conjunction with similar applications in the 1993 North Atlantic Regional Experiment (NARE) intensive and in the 1995 Southern Oxidants Study (SOS) Nashville/Middle Tennessee experiment [*Kleinman et al.*, 1997, 1998; *Daum et al.*, 2000], only a brief description is provided here. Input to the calculations includes the physical variables; time of day and date, UV solar intensity as observed from an Eppley radiometer, altitude, temperature, and dew point. Chemical variables used as model input were O_3, CO, NO, SO_2, HCHO, H_2O_2, organic peroxides, and speciated VOCs. As appropriate for a steady state box model calculation of an air parcel at midboundary layer altitude, there is no consideration of deposition, emissions, or transport. Model input data were averaged over 50 s time intervals, nearly matching the time resolution of the slowest chemical measurements. Fifty second averages of HCHO were calculated based on the assumption that HCHO concentrations were constant over a 3 min collection period. Geographic resolution of the urban plume was achieved by doing 12-19 calculations for each plume traverse, with the sample points spaced 1 or 2 minutes apart. The VOC data, in contrast to the other model inputs, were available only at a limited number of locations. In order to get the required geographic resolution we had to estimate VOC concentrations as discussed in section 5.

The chemical mechanism is based on the second-generation Regional Acid Deposition Model (RADM2) [*Stockwell et al.*, 1990] and on the condensed mechanism of *Paulson and Seinfeld* [1992] for isoprene. The reactive isoprene oxidation products, methyl vinyl ketone (MVK) and methacrolein (MACR) were not measured. Their concentrations are estimated to be 250 and 110% of isoprene, respectively, based on a steady state mixture governed by OH reaction kinetics. PAN is assumed to be in steady state. Photolysis rates are determined using the radiative transfer program of *Madronich* [1987] and climatological values for surface albedo, aerosol loading, and O_3 column. These values are then scaled to account for cloud cover using Eppley UV measurements from the G-1. This scaling is accomplished by comparing Eppley UV measurements on the day and time in question with clear-sky values taken at other times during the program.

5. Observations

We have selected four flights for a detailed study of conditions downwind of the city in the urban plume. On two of the flights (July 6 and 17) there was flow from the west or SW, which, as discussed in section 3, can cause the New York City plume to be superimposed upon a high regional pollutant background. Peak O_3 concentrations downwind of New York City were ~110 ppb based on both aircraft and surface observations. The other two flights on July 20 and 28 present an interesting contrast to July 6 and 17 in that winds were from the NW and the upwind region had fewer emission sources and lower pollutant concentrations. This resulted in lower O_3 levels (47-76 ppb) downwind, albeit at a distance that is closer to the city than the G-1 observations for July 6 and 17.

5.1. O_3, CO, and NO_y Measurements

Plate 2 shows the ground track of the G-1, color-coded to indicate O_3 concentration in the boundary layer portions of the four selected flights. On each plot the location of the urban plume is noted. A summary of winds and chemical concentrations is given in Table 1. Peak (1 minute average) concentrations of O_3, CO, and NO_y in the plumes are compared with the concentrations occurring in regions immediately adjacent to the plume, with the expectation that the difference tells us something about the effects of New York City emissions over and above whatever the background mix of pollutants is contributing to the plume and adjacent nonplume regions. Our tacit assumption is that the background is spatially uniform and thereby contributes equally to plume and adjacent nonplume regions.

Ozone production in the New York City plume, defined as the difference between plume and nonplume regions, is seen to be 31-34 ppb on W-SW flow days and 6-28 ppb on NW flow days. These values refer to the maximum O_3 concentrations observed from the G-1, which are not necessarily the absolute maximums occurring in the plume. They refer also to the particular conditions occurring on July 6, 17, 20, and 28, and will not be representative of all days with W-SW and NW flow. With these caveats in mind, some of the similarities and differences between the four flights are noted. The large difference between July 20 and 28 is due to the factor-of-5-larger wind speed on the July 20, which gives much better ventilation. However, a higher wind speed will cause the O_3 maximum on July 20 to appear farther downwind than on July 28, an effect we cannot assess with the available aircraft coverage. Ozone production on the July 28 is comparable to that on the July 6 and 17 despite the NW flow and the much cleaner upwind conditions. A contributing factor may be the lower wind speed on the July 28 and the additional time for O_3 production.

Another comparison that can be made using the data in Table 1 is between the plume and the region upwind of New York City. We take the upwind conditions to be representative of a regional background an hour or two before the New York City plume is being sampled. The background, so defined, has pollutant levels similar to the region adjacent to plume. Ozone production defined with respect to upwind conditions is 30-35 ppb for W-SW flow days and 12-38 ppb for NW flow days.

Surface level O_3 concentrations measured by an Environmental Protection Agency (EPA) network of monitoring stations are shown in Plate 3. Surface measurements are given at 1400 LST which is typically near the start of the midafternoon window when the O_3 plume from New York City has its maximum concentration and extent. The G-1 encounter with the urban plume took place ~2 h before the O_3 maximum on July 6 and close to the O_3 maximum on July 17. A comparison of the July 6 G-1 data with the surface observations (either at 1400 or at 1200 LST, not shown here) indicates that much of the New York City urban plume was located in Connecticut, north of the flight track. On July 17 the O_3 concentration remained high as the G-1 landed, implying that we might not have sampled the entire cross section of the plume. On July 20 and 28 the New York City plume was over the ocean, so that neither the timing nor the location of the plume encounter can be compared to surface observations.

The surface O_3 measurements clearly show that the region upwind of New York City under W-SW flow conditions can itself experience high O_3 concentrations. The highest O_3 concentrations in New Jersey on July 6 were 100-110 ppb, comparable to what was observed on the surface in Connecticut and what we observed in the New York City plume south of Long Island. This observation does not contradict our 71 ppb O_3 measurement on the July 6 upwind leg as that occurred ~5 hours before the New Jersey surface O_3 maximum. On July 17 the upwind stations in New Jersey recorded peak O_3 levels between 75 and 95 ppb, somewhat lower than that seen in Connecticut, but still indicating significant amounts of O_3 above clean background conditions.

5.2. VOC Concentrations

The hydrocarbon data are obtained from discrete canister samples and are sparse in comparison to the continuous trace gas measurements. In order to model the spatial variability of O_3 production across the plume we need to have input variables, in particular VOC concentrations, that resolve the spatial variability in O_3. In order to do this we rely on spatial patterns and/or the correlation of anthropogenic hydrocarbons with CO. Details of how this was done varied from day to day, as described below.

Our first step is to note that anthropogenic hydrocarbons are strongly correlated with CO. Using C_2H_2 as an example, a linear least squares regression yields the correlations: [CO (ppb)] = 111 + 0.26 [C_2H_2 (ppt)], $r^2 = 0.73$; total anthropogenic OH reactivity (s^{-1}) is equal to 0.03 + 0.0012 [C_2H_2(ppt)], $r^2 = 0.78$. Isoprene concentrations follow a spatial pattern dictated by the distribution of trees and other biogenic sources. For an OH concentration of 8×10^6 (representative of calculated values), the $1/e$ lifetime of isoprene is 20 min, leading to minimal transport from its source regions. Plate 4 shows isoprene concentrations measured within the boundary layer on all 15 flights. Concentrations are highly variable, even within a restricted geographic area. However, near zero concentrations were observed over eastern Long Island, Long Island Sound, and the Atlantic Ocean. The urban plumes depicted in Plate 2 are for the most part located in one of the near-zero isoprene regions, which makes the task of estimating isoprene concentrations less critical.

VOC sample coverage was relatively good on July 20 and 28, with five and six VOC samples, respectively, taken across the plume and adjacent nonplume regions, plus additional samples in upwind background air. Coverage was limited on July 6 and 17 with samples only in regions adjacent to the urban plume plus upwind samples on July 6. On the July 20 and 28, hydrocarbon concentrations at intermediate points across the plume were determined by linear interpolation using CO as an interpolation variable for the anthropogenic hydrocarbons and using a spatial interpolation for isoprene. On July 6 and 17 we used the correlations between CO and the individual hydrocarbons as observed over the entire experimental program to generate a synthetic hydrocarbon measurement. On both the July 6 and 17, isoprene concentrations were determined by geographic region, which resulted in near-zero (<10 ppt) concentrations in the over-water portions of the flights but concentrations as high as 160 ppt over Connecticut.

Figure 2 summarizes the hydrocarbon data for the plume, adjacent-to-plume, and upwind background regions, labeled P, A, and B, respectively. In order to take into account reactivity differences between the individual VOCs and to allow a comparison between CO, CH_4, HCHO, anthropogenic hydrocarbons, and isoprene the VOC data are presented in units of OH reactivity, defined for a single hydrocarbon by

$$VOC_i\ (s^{-1}) = k_i\ [VOC_i\ (ppb)] \quad (1)$$

where k_i is the rate constant for reaction of OH with VOC_i. The rate defined by (1) is the reciprocal of the lifetime of OH with respect to reaction with VOC_i. Isoprene reactivity includes contributions from its oxidation products, MVK and MACR. According to the assumed equilibrium with isoprene these products add an additional 82% to the reactivity of isoprene alone. The OH reactivity of a mixture is obtained by simply summing the components. Reactivity estimates determined from the VOC data are measures of the local photochemistry. They yield a description of the O_3 formation process at the point where the observations are made. Additional information is needed to determine which VOCs are responsible for the total excess O_3 in the urban plumes.

Figure 2 shows that the major components of plume reactivity are from CO and non-isoprene hydrocarbons (NIHC) with only a small contribution from isoprene. It is easy to understand this feature on July 6, 20, and 28, as the plume encounters were entirely over the Atlantic Ocean, where, as shown in Plate 4, isoprene concentrations are near zero. The data presented for July 17 are from the north shore of eastern Long Island and may have been influenced by flow from the Long Island sound. In contrast, isoprene is the largest contributor to reactivity in the background samples. The significance of even a small concentration of isoprene can be judged from the high background reactivities on July 6 and 28, which are due to 0.43 and 0.86 ppb isoprene, respectively.

It is likely that the plume in its earlier stages of evolution, closer to New York City, had a higher fraction of reactive ingredients. Therefore, closer to the emission source, the NIHC category would make a larger relative contribution to OH reactivity. A qualitative estimate of this effect can be obtained by considering the three VOC samples taken closest to the New York City source region (see Plate 4). The ratio of NIHC reactivity to concentration for these samples is 0.32-0.33 s^{-1} ppb C^{-1}. The corresponding ratio in the four plumes varies between 0.25 and 0.3 s^{-1} ppb C^{-1}, indicating that the aging which occurred in transport has led to a reactivity loss (per parts per billion Carbon) of up to 25%. This value does not, however, account for the aging that occurred from the point of emissions to our observation point at midboundary layer altitude.

5.3. Meteorology

It is difficult to provide a single measure of the winds as they vary with time, altitude, and geographic position. Around the coastal areas there are local effects due to sea breeze circulations. As one measure of the wind field, we have calculated back trajectories from the time and place of the O_3 maxima observed from the G-1. For this purpose we used the National Oceanic and Atmospheric Administration (NOAA) Hybrid Single-Particle Lagrangian Integrated Trajectory (HY-SPLIT) model driven by winds from the National Meteorological Center's Nested Grid Model [*Draxler*, 1992]. This model was accessed interactively from the World Wide Web server for the Air Resources Laboratory Node at http://www.arl.noaa.gov. Results in Table 1 are from isobaric trajectories at 500 m. Another measure of the wind direction is to simply note the location of the O_3 maximum relative to the region of maximum emissions in New York City. This measure is influenced by our flight path as the entire plume was not sampled on July 6 and possibly also on July 17. The surface O_3 network, specifically the location of sites measuring high O_3 is also useful (at least for July 6 and 17) in establishing the flow direction of the urban plume. There is reasonable agreement between these different wind measures.

Vertical profiles for the four flights indicated boundary layer heights between 1500 and 2000 m as specified in Table 1. UV radiometer measurements in and near the plumes indicated actinic fluxes that were between 90 and 100% of clear-sky values on the four flights.

5.4. Diagnostic Ratios

Table 2 shows the ratios CO/NO_y, O_3/NO_z, NO_x/NO_y, and H_2O_2/NO_z calculated from a data set consisting of the plume points and the adjacent nonplume regions. The first three ratios in Table 2 are determined as the slope of a least squares regression. By looking at a slope rather than the absolute value of the ratio we are eliminating some of the effects of background concentrations and focusing on the properties of the extra burden of pollutants in the plume relative to the adjacent nonplume area. For H_2O_2/NO_z and O_3/NO_z we give the actual value of the ratio in the plume so that we can compare our values with published values of indicator ratios.

5.4.1. CO/NO_y. The ratio CO/NO_y provides a useful test of an emission inventory if it can be determined that the ratio has not been affected by atmospheric processes. Of particular concern is depletion of NO_y due to dry deposition, which will increase the value of CO/NO_y as was sometimes observed to happen in the Nashville, Tennessee urban and power plant plumes [*Gillani et al.*, 1998a; *Nunnermacker et al.*, 1998, 2000]. The use of a regression method partially eliminates that concern as the regression slope is only sensitive to increases above background and is therefore not affected by deposition of background NO_y. In the context of our four flights this means that we only have to be concerned with deposition during the time that the air mass was transported from its source region near New York City. According to Table 1, transport times vary from 1.2 to 6 hours. Observations over a similar time span in Nashville [*Nunnermacker et al.*, 1998] showed up to a factor of 2 decrease in NO_y. The New York City data does not show evidence for rapid NO_y loss, as the CO/NO_y ratios do not systematically increase as travel times get longer. Consideration of weekday to weekend changes in the emission ratio, CO/NO_y (see below), does not change this conclusion.

Values of CO/NO_y on the four case study days range from 9 to 14. Emission ratios vary from place to place mainly because of different combinations of stationary and mobile sources. Table 2 includes an emission estimate from the Ozone Transport Assessment Group (OTAG) inventory for CO/NO_y from the core of the New York City metropolitan area, which we think is contributing most of the primary pollutants observed in the plumes. There is good agreement between emission ratio estimates and observations and even an indication that the observations follow the predicted weekday-weekend emission variation.

5.4.2. NO_x/NO_y. NO_x/NO_y is an indicator of the chemical age of an air mass; it qualitatively reflects the amount of chemical processing that has occurred due to reactions involving OH radical. This ratio starts out near unity in fresh emissions and monotonically decreases as NO and NO_2 are oxidized to products. This ratio tends to be very low in nonplume air, of the order of 0.1. Of the four plumes studied, the highest ratio occurs on July 28, consistent with the short 1.2 hour travel time from the New York

City source region. The other three cases have only 20-30% of the initial NO_x remaining. Although *Olszyna et al.* [1994] found that, for a rural atmosphere, the O_3 forming potential of an air mass is exhausted at about this NO_x to NO_y ratio, we find that there still can be a high rate of O_3 production because NO_x levels are high on an absolute basis. Whether this net chemical production leads to further increases in O_3 concentration depends on the nonchemical loss terms such as dilution due to diffusion and advection.

5.4.3. O_3/NO_z. The ratio O_3/NO_z, determined from the slope of a plot of O_3 versus NO_z is a measure of the efficiency at which photochemistry in the urban plume converts NO_x emissions into O_3 [*Trainer et al.*, 1993]. Given a NO_x emission rate, this ratio determines the resulting O_3. Table 2 indicates values ranging from 2.2 to 4.2. For comparison, values between 1 and 7 have been reported in plume studies during the 1995 SOS campaign in Nashville, Tennessee [*Meagher et al.*, 1998]; with the lower ratios generally occurring in large power plant plumes [*Ryerson et al.*, 1998; *Gillani et al.*, 1998b] and the higher ratios generally occurring at lower NO_x levels in small power plant plumes or in the Nashville urban plume [*St. John et al.*, 1998; *Valente et al.*, 1998; *Nunnermacker et al.*, 1998].

The O_3-NO_z concentration ratio has been used as an indicator for NO_x- and VOC-sensitive conditions on the basis of the modeling work of *Sillman* [1995]. Low values are associated with VOC-sensitive conditions, and high values are associated with NO_x-sensitive conditions. According to *Sillman's* northeast corridor results the transition between NO_x- and VOC-sensitive conditions occurs at about a ratio of 8, implying that O_3 formation in the New York City plume is VOC sensitive on July 6 and 17 and near the transition point to being NO_x sensitive on July 20 and 28. A more NO_x-sensitive chemistry on July 20 and 28 is in agreement with the larger relative contribution of NO_x-sensitive background O_3.

5.4.4. H_2O_2/NO_z. NO_x-sensitive chemistry tends to produce peroxides as an end product of the O_3 forming reactions while VOC-sensitive chemistry produces NO_z [*Sillman*, 1995; *Kleinman et al.*, 1997]. Low values of the ratio H_2O_2/NO_z therefore indicate VOC-sensitive conditions, and high values indicate NO_x-sensitive conditions. *Sillman's* northeast corridor calculations show that VOC-sensitive conditions occur when H_2O_2/NO_z is lower than ~0.2-0.5, implying that O_3 formation in the New York City plume is VOC sensitive.

6. Discussion

In this section we take a closer look at trace gas concentrations in the plume and adjacent nonplume regions, combining this information with results obtained from the constrained steady state photochemical calculations. The top and middle plots of Figures 3-6 show the concentrations of O_3, CO, NO_y, and NO_x on July 6, 17, 20, and 28. In the bottom plots of Figures 3-6 we show calculated results, namely the O_3 production rate $P(O_3)$ and the fraction of odd hydrogen free radicals being removed by reactions with NO_x, L_N/Q. Points on the graphs are spaced 1 or 2 min apart except for those times where instruments were in zero mode.

The combination of $P(O_3)$ and L_N/Q quantifies the photochemical activity of the air mass and tells us where it is in the natural progression from being VOC sensitive near a large urban source region to being NO_x sensitive far away [*Staffelbach et al.*, 1997; *Sillman*, 1999]. We rely on previous work that shows the relation between L_N/Q and the relative sensitivity of $P(O_3)$ to changes in the concentrations of NO_x and VOCs [*Kleinman et al.*, 1997]. As a follow-on step, we present a qualitative argument that relates the $P(O_3)$ sensitivities to quantities that are more directly related to emission controls.

6.1. Plume Source and Structure

There are several lines of evidence indicating that the observed plumes are indeed coming from the New York City metropolitan area. That area, as indicated by the middle box in Plates 1a and 1b, has the highest emission rates and emission densities in an extended region, so therefore if the viewing geometry is correct, the largest, most intense plume should be attributable to the New York City metropolitan area. This assignment is consistent with the trajectory directions shown in Table 1, which are within 18° of the direction obtained by drawing a line from the observed O_3 peak to the city center. Also, the ratio of NO_x to NO_y is consistent with the plume travel times shown in Table 1. Photochemical calculations indicate late morning to early afternoon values of [OH] of ~0.9 to 1.3×10^7 molecules cm^{-3}. A nearby NO_x source 1 h from the observed plume would yield a NO_x to NO_y ratio of 72%, assuming an [OH] of 1×10^7. This is close to what was observed on July 20, but rules out a major (but not a minor) contribution from nearby NO_x sources on the other three days. A large NO_x contribution from much farther upwind is also unlikely, on the basis of upwind NO_y measurements and again on OH estimates. For example, six hours of transport with an [OH] of 1×10^7 would yield a NO_x to NO_y ratio of 14%, which is lower than observed. Finally, on July 6 there is direct evidence of the source region, as the G-1 made additional traverses showing elevated CO and NO_y (NO_x not available) closer to the city.

The plumes on July 17, 20, and 28 (Figures 4-6) have structure that reflects a combination of spatial inhomogeneities in the source region and inhomogeneities in the transporting wind field. In the absence of a mesoscale analysis of the 3-D wind fields we cannot reach any definitive conclusions regarding the origin of the plume structure. We will, however, point out several features and provide hypotheses for their origin.

On July 17 and 28 the urban plume has two peaks separated by a region with near-background levels of O_3, NO_y, and CO. The ratio of NO_x to NO_y in the interpeak region is particularly low, around 5%, suggesting the absence of a recent emission input. It is difficult to reconcile a background-like plume segment with a uniform advecting wind field because the upwind region does not contain any very low emission gaps. It appears that the New York City plume has bifurcated, perhaps because of vertical wind shear, leaving a relatively undisturbed region in the middle.

On July 20 the concentration data indicate that CO, NO_y, and NO_x are correlated but have a peak that is well displaced from the peak in O_3. The same thing occurs, but to a lesser extent, on the second peak on July 28. We believe this to be a geometric effect whereby part of the urban plume was impacted by nearby sources on Long Island. These sources contribute NO_x and CO, but a lesser amount of O_3 is formed from them because the processing time is less than it is for emissions originating in the center of New York City. The plume traverses on July 6 and 17 must also be measuring a mixture of pollutants including a relatively fresh component from sources downwind of New York City. There is no apparent signature for these more local emissions because they

are superimposed on the main New York City metropolitan area emissions in a way that does not stand out. We see the younger emissions on July 20 and 28 only because the Long Island sources are to one side of the main plume.

6.2. O_3 Production Rate

In Figure 7 we plot calculated $P(O_3)$ for four days as a function of NO concentration. Points adjacent to the urban plume are at low [NO], while the plume points are to the right at higher [NO]. There are several features of this graph which can be explained with reference to previous studies which examined the dependence of $P(O_3)$ on NO_x and VOC concentrations [*Daum et al.*, 2000; *Kleinman et al.*, 1995, 1997; *McKeen et al.*, 1991; *Sillman et al.*, 1990, 1995].

At low NO_x an approximate but fairly accurate (of the order of 10% errors) formula for $P(O_3)$ is

$$P(O_3) = k_t/(2k_{eff})^{1/2}\, Q^{1/2}\, [NO], \qquad (2)$$

where k_t is the average rate constant for HO_2, RO_2 + NO, k_{eff} is an effective rate constant for peroxide formation, and Q is the rate of radical production [*Kleinman et al.*, 1995]. Equation (2) predicts a linear dependence of $P(O_3)$ on [NO], which is what Figure 7 shows at NO concentrations below 0.2 ppb (NO_x lower than ~1 ppb). There is some scatter to this relation, caused mainly by variations in Q, which is driven in part by day to day differences in O_3 concentration. At higher values of [NO], $P(O_3)$ is much lower than would be predicted from an extrapolation of the linear low-NO trend. This behavior is due to the increasing role of NO_x as a radical scavenger as can be seen from the following relation, which is valid at low and high NO_x [*Kleinman et al.*, 1997; *Daum et al.*, 1999]:

$$P(O_3) = k_t/(2k_{eff})^{1/2}\, Q^{1/2}(1\text{-}L_N/Q)\, [NO] \qquad (3)$$

Note that (2) follows from (3) by taking the limit that $L_N/Q \rightarrow 0$, which happens at low NO_x concentrations. Although (3) describes $P(O_3)$ with about a 10% accuracy, it is not very useful at high NO_x because L_N/Q approaches 1 as [NO] gets large, so the limiting behavior of $(1\text{-}L_N/Q)$[NO] is not apparent. A more transparent high-NO_x formula is

$$P(O_3) = Y\,(k_1\,[VOC]/k_2\,[NO_2])\,Q \qquad (4)$$

where Y is the average number of peroxy radicals formed after OH + VOC; k_1 is an average rate constant for OH + VOC; and k_2 is the rate constant for OH + NO_2 [*Sillman*, 1995; *Daum et al.*, 2000]. Figure 8 indicates that day to day differences in $P(O_3)$ for high-NO_x points can be related to the variables on the right-hand side of (4). A closer look at what is driving the differences between July 6, 20, and 28 reveals that the VOC to NO_2 reactivity ratio is about the same on these three days, but the radical production rate Q varies by a factor of 2.5 in response to differences in O_3 and HCHO. The import of these compounds from upwind of the city can thereby lead to an increase in $P(O_3)$ downwind of the city.

6.3. O_3 Production Rate Sensitivity

The sensitivity of $P(O_3)$ to changes in the concentration of NO or hydrocarbons is evaluated by running a constrained steady state calculation with perturbed values of either NO or hydrocarbons and comparing the calculated $P(O_3)$ with a base case value. It is convenient to look at relative sensitivities, i.e.,

$$\frac{d\ln P(O_3)}{d\ln [NO]} = \frac{[NO]}{P(O_3)}\,\frac{dP(O_3)}{d[NO]}, \qquad (5)$$

where the derivative is calculated numerically from the change in $P(O_3)$ after [NO] is perturbed by some small amount (10% in these calculations). A similar expression applies for dln $P(O_3)$/dln [VOC] with the derivative being evaluated for a 10% change in CH_4, CO, isoprene, and anthropogenic VOCs. The relative sensitivities are defined such that they have a value of 1 when a n% change in NO or VOCs produces a n% change in $P(O_3)$. As discussed by *Kleinman et al.* [1997] and *Kleinman* [2000], relative sensitivities of $P(O_3)$ give information on the instantaneous response of the atmosphere to changes in [NO] and [VOC]. These quantities should not be confused with the emission control factors, dln $[O_3]$/dln E_{NO} or E_{VOC}, which specify the response of O_3 concentration to a change in emissions (E_{NO} or E_{VOC}) at some upwind location in the past. Relative sensitivities do, however, provide qualitative information on emission controls as explored in section 6.4.

In Figure 9 we show relative sensitivities as a function of the process variable L_N/Q, the fraction of free radicals which are removed by reacting with NO_x. The bottom plots in Figures 3-6 show the variation of L_N/Q across the urban plume. The solid lines in Figure 9 are analytic expressions from *Kleinman et al.* (1997),

$$\frac{d\ln P(O_3)}{d\ln [NO]} = \frac{1 - 3/2\, L_N/Q}{1 - 1/2\, L_N/Q}, \qquad (6)$$

$$\frac{d\ln P(O_3)}{d\ln [HC]} = \frac{1/2\, L_N/Q}{1 - 1/2\, L_N/Q}, \qquad (7)$$

which are seen to qualitatively represent the numerical calculations. Points in the urban plumes have L_N/Q values mostly greater than 0.7. Both the analytic formula and numerical results agree that in the urban plume, $d$ln P/dln [NO] is negative, meaning that an [NO] increase leads to a smaller value of $P(O_3)$. For these points a decrease in VOCs is the only way to decrease $P(O_3)$. Background points have low values of L_N/Q, and for those points, reducing VOCs does not do much to change $P(O_3)$, but a reduction in [NO] is accompanied by a nearly proportional reduction in $P(O_3)$. The L_N/Q axis spans the range from strongly NO_x sensitive on the left, to a crossover point in the middle and strongly VOC sensitive on the right.

The centers of the urban plumes are VOC sensitive, sometimes strongly so with L_N/Q approaching 1. This is noteworthy because these determinations, at least for July 6 and 17, are made near the time and place where, according to surface observations, the maximum O_3 occurs. Again, we caution that the designation "NO_x or VOC sensitive" refers here to the instantaneous O_3 production rate.

6.4. Emission Controls

On a given day, plume observations are made at a single downwind distance. We can calculate the sensitivity of $P(O_3)$ to changes in NO and VOCs at that single distance, but by itself this does not tell us much about the response of O_3 to changes in emissions, which depends upon the entire history of the air mass. We

would be closer to the goal of determining a response to an emission control if we knew the local sensitivities of $P(O_3)$ as a function of time from the source region to the point where we make our observations. For example, if $P(O_3)$ was strongly VOC sensitive at all points between emission and observation, it is likely that O_3 concentration would also be VOC sensitive because we know in some general sense that O_3 concentration must be built up out of $P(O_3)$ as the air mass evolves. The situation is actually somewhat more complicated. While O_3, in the absence of chemical loss and dilution, can be expressed as a time integral of the local quantity $P(O_3)$, i.e.,

$$O_3 = \int P(O_3)\, dt \ , \qquad (8)$$

it is not true that the response of O_3 to an emissions change can likewise be determined from local quantities, i.e.,

$$dO_3/dE(\mathrm{VOC}) \neq \int dP(O_3)/d[\mathrm{VOC}]\, dt \ , \qquad (9)$$

because the latter integral does not take into account the possible nonlinear response of [VOC(t)] to an emission change. Nevertheless, we proceed on the plausible assumption that a system that is always strongly VOC sensitive in the instantaneous sense will be VOC sensitive in the integral sense.

The problem, then, is to determine the likely past history of an air mass given a single downwind observation. We take as our starting point the data gathered on the plume traverses, using the July 6 observations as an example. Upwind conditions are not known, but we can assume that the plume was more concentrated and had higher VOCs and NO_x, but lower O_3. We have done a series of calculations increasing either NO_x or VOCs or both. We also consider the effect of reducing O_3 by itself and in combination with an increase in NO_x and VOCs. These calculations show how the instantaneous sensitivity of $P(O_3)$ evolves as an air mass moves away from its source region.

Information on the NO_x and VOC sensitivities of the base case and perturbed scenarios is contained in the variable L_N/Q, which is shown in Figure 10. We choose to look at L_N/Q rather than $d\ln P(O_3)/d\ln$ [NO or VOC] for each of the scenarios because it is somewhat easier to interpret and because Figure 9 indicates that it is a reasonable surrogate. Figure 10 shows that a doubling of NO_x increases L_N/Q and thereby makes the system more VOC sensitive. As L_N/Q is the fraction of radicals removed by reaction with NO_x, it is expected that it would increase as NO_x concentrations increase. A doubling of [VOC], according to Figure 10, has the opposite effect of decreasing L_N/Q and making the system more NO_x sensitive. This result follows from the fact that the major contributor to L_N is from the reaction of OH with NO_2, and that increasing [VOC] tends to decrease [OH].

When both NO_x and VOCs are doubled the increase in NO_x has the stronger effect; L_N/Q increases, and the atmosphere becomes more VOC sensitive. It takes only a 25% increase in NO_x to counterbalance a 100% increase in VOCs and leave L_N/Q unchanged. As we look backward in time we expect that the NO_x to VOC ratio in the plume increases because NO_x is more reactive than the average VOC. This effect by itself causes plumes to evolve from being more VOC sensitive near their source to being more NO_x sensitive downwind [*Sillman*, 1993, 1999; *Staffelbach et al.*, 1997; *Duncan and Chameides*, 1998]. We show here that the tendency to be VOC sensitive near the source is even stronger than can be explained by a change in NO_x to VOC ratio. Even if the NO_x to VOC ratio stays the same, our calculations show that L_N/Q increases, and the plume becomes more VOC sensitive. This is an example of an effect discussed by *Sillman* [1999] whereby more polluted conditions (i.e., with higher concentrations of both NO_x and VOCs) tend to be more VOC sensitive. We have also done calculations in which we consider the effects of a lower upwind O_3 concentration. Allowing O_3 to vary does not change the conclusion that the plume is more VOC sensitive near its source region. Having established that $P(O_3)$ is VOC sensitive at all points between the source region and the place where the plume is intercepted, we conclude that O_3 formed in the plume is more sensitive to VOC emissions than to NO_x emissions.

Photochemical model calculations [*Rao and Sistla*, 1993; *Roselle et al.*, 1991; *National Research Council*, 1991, pp. 362-375; *Roselle and Schere*, 1995; *Sistla et al.*, 1996] for the NE corridor indicate that O_3 in the New York City metropolitan area is best controlled by VOC reductions, at least in the case of the worst O_3 episodes. This sensitivity, determined from model predictions, pertains to a combination of O_3 formed in the New York City urban plume as well as background O_3 imported into the area. Our finding of VOC sensitivity pertains only to O_3 formed in the urban plume, which we expect will be more VOC sensitive than total O_3 [e.g., *Sillman*, 1999]. However, whereas models indicate a transition to NO_x sensitivity under less polluted conditions [*Roselle and Schere*, 1995], our results show that O_3 formed in the urban plume remains VOC sensitive even at O_3 levels of 50-110 ppb.

7. Conclusions

Downwind traverses of the New York City urban plume by the DOE G-1 airplane showed that 31-34 ppb of O_3 was produced 3-4 hours downwind on 2 days (July 6 and 17) having W-SW winds. Ozone levels of ~110 ppb resulted. On 2 days, July 20 and 28, with NW winds, O_3 production was 6 and 28 ppb, leading to O_3 levels of 41 and 76 ppb at locations 1 and 5 hours downwind of the source region, respectively. High wind speed on July 20 accounted for it being much cleaner than July 28. Differences in downwind O_3 between W-SW and NW flow conditions are accounted for by the location of emission sources, which leads to higher pollutant levels being imported into the New York City metropolitan area when flow is from the W-SW, along the northeast corridor. Surface O_3 observations from the EPA monitoring network indicated that on the 2 days with W-SW flow the G-1 intercepted the urban plume close to the time and place where maximum O_3 occurred. This is the place where it is most important to determine whether O_3 control is best done using NO_x or VOC reductions.

The W-SW plumes were observed 110 km downwind of New York City at which point they had experienced 3-4 hours of aging. Most of the NO_x from the urban area had reacted away, leaving a NO_x to NO_y ratio of 20-30%. Peak NO_x concentrations were 7 ppb on July 6 and 4 ppb on July 17, sufficient to support an active photochemistry and, furthermore, as several lines of reasoning indicate, high enough to cause O_3 formation to be VOC sensitive.

A comparison of VOC-OH reactivity in the urban plume with that observed in background air, upwind of the New York City metropolitan area, indicates that the plume and background have comparable reactivity. The plume has a higher concentration of CO and anthropogenic hydrocarbons, but the background air has a higher concentration of isoprene. Low isoprene in the urban plume was due to its location, over or near bodies of water. Relatively

low VOC levels contribute to the VOC limitation on O_3 production.

A comparison between the observed ratio of CO to NO_y in the urban plume and an emission ratio determined from the OTAG inventory for the center of the New York City metropolitan area indicates agreement of the ratios to within 20%. The inventory gives a ratio of 8.2 and 10.8 for weekdays and weekends, respectively. The corresponding observed values are 8.8 and 12.7. There are no large systematic changes in the value of CO/NO_y with respect to plume age that would indicate rapid deposition of NO_y such as was seen in Nashville, Tennessee.

The ratio of O_3 to NO_z in the urban plumes had values between 5.4 and 9.4; H_2O_2/NO_z had values between 0.08 and 0.2. According to calculations by *Sillman* [1995] the H_2O_2 to NO_z ratios are all within the range of values associated with O_3 being VOC sensitive. The O_3 to NO_z ratios show VOC-sensitive conditions on July 6 and 17 and conditions near the VOC to NO_x transition point on the other 2 days, consistent with a larger relative contribution of NO_x-sensitive background O_3 on July 20 and 28. Ozone production efficiencies determined from the slope of an O_3-NO_z regression had values between 2.2 and 4.2.

Steady state photochemical calculations were performed using plume observations as constraints. These calculations yield the production rate of O_3, $P(O_3)$, the fraction of free radicals which are removed by reacting with NO_x, L_N/Q, and the sensitivity of $P(O_3)$ to changes in the concentrations of NO or VOCs, $d\ln P(O_3)/d\ln$ [NO or VOC]. Maximum values of $P(O_3)$ were 14 and 12 ppb h^{-1}, on July 6 and 17, respectively, indicating a still active photochemistry after 3-4 hours of aging. These high values for $P(O_3)$ were observed in regions where O_3 concentrations were within 10 ppb of their maximum values as indicated by the surface monitoring network. Evidently, at these locations there is almost a balance between gain of O_3 by chemical production and loss by dispersion. In as much as the O_3 maximums occur in regions where NO_x/NO_y is about 20-30%, our results agree with the findings of *Olszyna et al.* [1994] that maximum O_3 concentrations are reached at about that point. On one of the days with NW winds (July 28), maximum $P(O_3)$ was only slightly lower, 11 ppb h^{-1}. This is consistent with the observation that the O_3 increase (relative to the adjacent nonplume regions) on July 28 was only slightly less than that seen on July 6 and 17.

In all four urban plumes, $P(O_3)$ is VOC sensitive, meaning that $P(O_3)$ is more sensitive to a small fractional change in [VOC] than it is to the same small fractional change in [NO]. In three of the plumes, NO_x inhibits O_3 production; that is, $P(O_3)$ increases when NO is decreased. As shown in previous work, the $P(O_3)$ sensitivities are well represented by simple analytic formulas that depend only on L_N/Q [*Kleinman et al.*, 1997]. Low- and high-NO_x formulas for $P(O_3)$ reproduce its dependence on NO_x, VOCs, and radical production rate.

$P(O_3)$ sensitivities are local properties of an air mass, whereas the sensitivity of O_3 concentration to an emissions change depends on the history of an air mass from the point of emissions to the point where it is being observed. A plausible, but not mathematically rigorous, argument was constructed to show how $P(O_3)$ sensitivities are related to the effects of emission controls. It was argued that if the instantaneous $P(O_3)$ is VOC sensitive at every point in the history of an air mass, it is likely that the integrated O_3 will also be VOC sensitive. It was further argued that closer to the source region (i.e., looking back in time) an air mass would have a higher NO_x and VOC concentration and the ratio of NO_x to VOC would either be the same or higher. For this hypothetical but physically reasonable set of conditions the steady state calculations show that $P(O_3)$ becomes more VOC sensitive close to the emission source region. Therefore $P(O_3)$ is VOC sensitive over the whole history of the air mass, and O_3 itself is VOC sensitive. This argument is based on calculations which consider the effects of small perturbations. The problem of NO_x and VOC sensitivity has to be addressed also from the perspective of the large emission changes which Eulerian models indicate are necessary to meet air pollution standards [*Roselle and Schere*, 1995].

Acknowledgment. We thank the pilots and flight crew from PNNL for a job well done. We gratefully acknowledge the many contributions of P. Doskey of ANL, P. Klotz of BNL, and C. Berkowitz, J. Hubbe, and V. Morris of PNNL in collecting and reducing the data. We thank S. Sillman of the University of Michigan and G. Sistla of the New York State Department of Environmental Conservation for providing emission estimates. This study benefitted in many ways from the framework that was provided by the NARSTO-NE 1996 Summer Ozone Study. We gratefully acknowledge the support of the Atmospheric Chemistry Program within the Office of Biological and Environmental Research of DOE for providing the G-1 aircraft. In addition to DOE, support for participation in the NARSTO-NE intensive was from EPRI under contract WO 9108-20. L. Kleinman gratefully acknowledges support from P. Mueller of EPRI for modeling and data analysis. This research was performed under sponsorship of the U.S. DOE under contracts DE-AC02-98CH10886.

References

Berkowitz, C. M., J. D. Fast, S. R. Springston, R. J. Larsen, C. W. Spicer, P. V. Doskey, J. H. Hubbe, and R. Plastridge, Formation mechanisms and chemical characteristics of elevated photochemical layers over the northeast United States, *J. Geophys. Res.*, *103*, 10,631-10,647, 1998.

Blumenthal, D. L., F. W. Lurmann, N. Kumar, T. S. Dye, S. E. Ray, and M. E. Korc, Transport and mixing phenomena related to ozone exceedances in the northeast U.S. (analysis based on NARSTO-northeast data), *Working Draft 1, STI-996133-1710-WD1*, Sonoma Technol., Santa Rosa, Calif., 1997.

Chameides, W. L, and E. B. Cowling, The state of the Southern Oxidants Study: Policy-relevant findings in ozone pollution research, 1988-1994, South. Oxidants Study, Coll. of For. Resour., N. C. State Univ., Raleigh, 1995.

Chameides, W. L., R. W. Lindsay, J. Richardson, and C. S. Kiang, The role of biogenic hydrocarbons in urban photochemical smog: Atlanta as a case study, *Science*, *241*, 1473-1475, 1988.

Daum, P. H., L. Kleinman, D. G. Imre, L. J. Nunnermacker, Y.-N. Lee, S. R. Springston, and L. Newman, Analysis of the processing of Nashville urban emissions on July 3 and July 18, 1995, *J. Geophys. Res.*, in press, 2000.

Draxler, R. R., Hybrid single-particle Lagrangian integrated trajectories (HY-SPLIT): Version 3.0 users guide and model description, *NOAA Tech. Memo. ERL ARL-195*, *Natl. Oceanic and Atmos. Admin.*, Washington, D. C., 1992.

Duncan, B. N., and W. L. Chameides, Effects of urban emission control strategies on the export of ozone and ozone precursors from the urban atmosphere to the troposphere, *J. Geophys. Res.*, *103*, 28,159-28,179, 1998.

Gillani, N. V., M. Luria, R. J. Valente, R. L. Tanner, R. E. Imhoff, and J. F. Meagher, Loss rate of NO_y from a power plant plume based on aircraft measurements, *J. Geophys. Res.*, *103*, 22,585-22,592, 1998a.

Gillani, N. V., J.F. Meagher, R. J. Valente, R. E. Imhoff. R. L. Tanner, and M. Luria, Relative production of ozone and nitrates in urban and rural power plant plumes, 1, Composite results based on data from 10 field measurement days, *J. Geophys. Res.*, *103*, 22,593-22,615, 1998b.

Kleinman, L. I., Ozone process insights from field experiments, part II, Observation based analysis for ozone production, *Atmos. Environ.*, in press, 2000.

Kleinman, L. I., P. H. Daum, J. H. Lee, Y.-N. Lee, J. Weinstein-Lloyd, S. R. Springston, M. Buhr, and B. T. Jobson, Photochemistry of O_3 and related compounds over southern Nova Scotia, *J. Geophys. Res.*, *103*, 13,519-13,529, 1998.

Kleinman, L. I., P. H. Daum, J. H. Lee, Y.-N., Lee, L. J. Nunnermacker, S. R. Springston, L. Newman, J. Weinstein-Lloyd, and S. Sillman, Dependence of ozone production on NO and hydrocarbons in the troposphere, *Geophys. Res. Lett., 24*, 2299-2302, 1997.

Kleinman, L. I., P. H. Daum, S. R. Springston, W. R. Leaitch, C. M. Banic, G. A. Isaac, T. Jobson, and H. Niki, Measurement of O_3 and related compounds over southern Nova Scotia, 2, Photochemical age and vertical transport, *J. Geophys. Res.*, *101*, 29,061-29,074, 1996.

Kleinman, L., Y.-N. Lee, S. R. Springston, J. H. Lee, L. Nunnermacker, J. Weinstein-Lloyd, X. Zhou, and L. Newman, Peroxy radical concentration and ozone formation rate at a rural site in the southeastern United States, *J. Geophys. Res.*, *100*, 7263-7273, 1995.

Lee, Y.-N., X. Zhou, W. R. Leaitch, and C. M. Banic, An aircraft measurement technique for formaldehyde and soluble carbonyl compounds, *J. Geophys. Res.*, *101*, 29,075-29,080, 1996.

Lehrman, D., W. R. Knuth, and N. L. Alexander, 1996 rawinsonde measurements, version 1.0, *EPRI TR-109526*, Electr. Power Res. Inst., Palo Alto, Calif., June 1997a.

Lurmann, F. W., N. Kumar, R. Londergan, and G. Moore, Evaluation of the UAM-V model performances in the northeast region of OTAG episodes, *Working Draft 2.1, STI-996133-1716-WD2.1*, Sonoma Technol., Santa Rosa, Calif., 1997.

Madronich, S., Photodissociation in the atmosphere, 1, Actinic flux and the effects of ground reflections and clouds, *J. Geophys. Res.*, *92*, 9740-9752, 1987.

McKeen, S. A., E. Y. Hsie, and S. C. Liu, A study of the dependence of rural ozone on ozone precursors in the eastern United States, *J. Geophys. Res.*, *96*, 15,377-15,394, 1991.

Meagher, J. F., E. B. Cowling, F. C. Fehsenfeld, and W. J. Parkhurst, Ozone formation and transport in southeastern United States: Overview of the SOS Nashville/Middle Tennessee Ozone Study, *J. Geophys. Res.*, *103*, 22,213-22,223, 1998.

National Research Council, *Rethinking the Ozone Problem in Urban and Regional Air Pollution*, Natl. Acad. Press, Washington, D. C., 1991.

Nunnermacker, L. J., L. Kleinman, D. Imre, P. H. Daum, Y.-N. Lee, J. H. Lee, S. Springston, and L. Newman, NO_y lifetimes and O_3 production efficiencies in urban and power plant plumes: Analysis of field data, *J. Geophys. Res.*, in press, 2000.

Nunnermacker, L. J., et al., Characterization of the Nashville urban plume on July 3 and July 18, 1995, *J. Geophys. Res.*, *103*, 28,129-28,148, 1998.

Olszyna, K. J., E. M. Bailey, R. Simonaitis, and J. F. Meagher, O_3 and NO_y relationships at a rural site, *J. Geophys. Res.*, *99*, 14,557-14,563, 1994.

Paulson, S. E., and J. H. Seinfeld, Development and evaluation of a photochemical mechanism for isoprene, *J. Geophys. Res.*, *97*, 20,703-20,715, 1992.

Rao, S. T., and G. Sistla, The efficacy of nitrogen oxides emissions control in ozone attainment strategies as predicted by the urban airshed model, *Int. J. Air Water Soil Pollut.*, *67*, 95-116, 1993.

Ray, S. E., T. S. Dye, C. G. Lindsey, and M. Arthur, 1996 upper-air and surface meteorological data, version 1.0, *EPRI TR-109528*, Electr. Power Res. Inst., Palo Alto, Calif., June 1997.

Roberts, P., M. Korc, and D. Blumenthal, NARSTO-Northeast 1996 Summer Ozone Study, version 1.0, *EPRI WO9108-01*, Electr. Power Res. Inst., Palo Alto, Calif., December 1996a.

Roberts, P., M. Korc, and D. Blumenthal, EPRI, 1996 field plan protocol, version 1.0, *EPRI TR-109538*, Electr. Power Res. Inst., Palo Alto, Calif., June, 1996b.

Roselle, S. J., and K. L. Schere, Modeled response of photochemical oxidants to systematic reductions in anthropogenic volatile organic compound and NO_x emissions, *J. Geophys. Res.*, *100*, 22,929-22,941, 1995.

Roselle, S. J., T. E. Pierce, and K. L. Schere, The sensitivity of regional ozone modeling to biogenic hydrocarbons, *J. Geophys. Res.*, *96*, 7371-7394, 1991.

Ryan, W. F., B. G. Doddridge, R. R. Dickerson, R. M. Morales, K. A. Hallock, P. T. Roberts, D. L. Blumenthal, J. A. Anderson, and K. L. Civerolo, Pollutant transport during a regional O_3 episode in the Mid-Atlantic states, *J. Air Waste. Manage. Assoc.*, *48*, 786-797, 1998.

Ryerson, T. B., et al., Emissions lifetimes and ozone formation in power plant plumes, *J. Geophys. Res.*, *103*, 22,569-22,583, 1998.

Sillman, S., D. He, C. Cardelino, and R. E. Imhoff, The use of photochemical indicators to evaluate ozone-NO_x-hydrocarbon sensitivity: Case studies from Atlanta, New York and Los Angeles, *J. Air Waste Manage. Assoc.*, *47*, 1030-1040, 1997.

Sillman, S., J. A. Logan, and S. C. Wofsy, The sensitivity of ozone to nitrogen oxides and hydrocarbons in regional ozone episodes, *J. Geophys. Res.*, *95*, 1837-1851, 1990.

Sillman, S., Review article: The relation between ozone, NO_x and hydrocarbons in urban and rural environments, *Atmos. Environ.*, *33*, 1821-1845, 1999.

Sillman, S., The use of NO_y, H_2O_2, and HNO_3 as indicators for ozone-NO_x-hydrocarbon sensitivity in urban locations, *J. Geophys. Res.*, *100*, 14,175-14,188, 1995.

Sillman, S., Tropospheric ozone: The debate over control strategies, *Annu. Rev. Energy Environ., 18*, 31-56, 1993.

Sistla, G., N. Zhou, W. Hou, J.-Y. Ku, S. T. Rao, R. Bornstein, F. Freedman, and P. Thuns, Effects of uncertainties in meteorological inputs on Urban Airshed Model predictions and ozone control strategies, *Atmos. Environ.*, *30*, 2011-2025, 1996.

St. John, J. C., W. L. Chameides, and R. Saylor, Role of anthropogenic NO_x and VOC as ozone precursors: A case study from the SOS Nashville/Middle Tennessee Ozone Study, *J. Geophys. Res.*, *103*, 22,415-22,423, 1998.

Staffelbach, T., A. Neftel, and L. W. Horowitz, Photochemical oxidant formation over southern Switzerland, 2, Model results, *J. Geophys. Res.*, *102*, 23,363-23,373, 1997.

Stockwell, W. R., P. Middleton, J. S. Chang, and X. Tang, The second generation regional acid deposition model chemical mechanism for regional air quality modeling, *J. Geophys. Res.*, *95*, 16,343-16,367, 1990.

Trainer, M., et al., Correlation of ozone with NO_y in photochemically aged air, *J. Geophys. Res.*, *98*, 2917-2925, 1993.

U. S. Environmental Protection Agency (EPA), Regional interim emission inventories (1987-1991), *EPA-454/R93-021a and b*, vol. I and II, Research Triangle Park, N. C., 1993.

Valente, R. J., R. E. Imhoff, R. L. Tanner, J. F. Meagher, P. H. Daum, R. M. Hardesty, R. M. Banta, R. J. Alvarez, R. T. McNider, and N. V. Gillani, Ozone production during an urban air stagnation episode over Nashville, Tennessee, *J. Geophys. Res.*, *103*, 22,555-22,568, 1998.

Weinstein-Lloyd, J. B., P. H. Daum, L. J. Nunnermacker, J. H. Lee, and L. I. Kleinman, Measurement of peroxides and related species in the 1993 North Atlantic Regional Experiment, *J. Geophys. Res.*, *101*, 29,081-29,090, 1996.

Zhang, J., S. T. Rao, and S. M. Daggupta, Meteorological processes and ozone exceedances in the northeastern United States during the 12-16 July 1995 episode, *J. Appl. Meteorol.*, *37*, 776-789, 1998.

P. H. Daum, D. G. Imre, L. I. Kleinman, J. H. Lee, Y.-N. Lee, L. Newman, L. J. Nunnermacker, S. R. Springston, and J. Weinstein-Lloyd, Atmospheric Sciences Division, Brookhaven National Laboratory, P. O. Box 5000, Upton, NY 11973-5000. (phdaum@bnl.gov; imre@bnl.gov; kleinman@bnl.gov; ynlee@bnl.gov; newman@bnl.gov; lindan@bnl.gov; srs@bnl.gov; jlloyd@bnl.gov.)

Table 1. Plume Characteristics

Variable	July 6	July 17	July 20	July 28
Time of day, LST	1125	1450	1345	1345
Wind at 500 m from trajectory				
Speed, km/h	33	27	50	11
Direction, deg	250	279	298	297
Upwind concentration				
O_3 (ppb)	71	80[a]	35	38
CO (ppb)	228		115	154
NO_y (ppb)	9.6[b]		2.9	2.7
Concentrations adjacent to plume				
O_3 (ppb)	75	76	41	48
CO (ppb)	190	170	135	170
NO_y (ppb)	8	11	4	6
Peak downwind conc.[c]				
O_3 (ppb)	106	110	47	76
CO (ppb)	395	263	211	382[d]
NO_y (ppb)	26.3	22.3	9.6	16.5
Travel time from New York City to peak, h	3.2	4.1	1.2	4.9-5.8
Direction from New York City to peak, deg	268	261	293	287-348
Boundary layer height, m	1500	1700	2000	1900

[a]Estimated from surface observations.
[b]Few data points.
[c]One minute averages. Peak concentrations of O_3, CO, and NO_y do not necessarily occur at the same location.
[d]CO in zero mode at peak, extrapolated from local CO:NO_y relation.

Table 2. Derived Plume Characteristics

Variable	July 6	July 17	July 20	July 28
Observed				
CO/NO_y[a]	11.1 (0.90)	8.8 (0.93)	13.9 (0.75)	13.1 (0.75)
O_3/NO_z[a]	2.2 (0.91)	3.8 (0.93)	4.2 (0.75)	4.0 (0.84)
NO_x/NO_y[a]	0.30 (0.97)	0.22 (0.74)	0.65 (0.95)	0.29 (0.71)
H_2O_2/NO_z[b]	0.08	0.15	0.2	0.15
O_3/NO_z[b]	5.4	6.3	9.4	8.5
Emission Inventory				
CO/NO_y	10.6	8.2	10.6	11.0
Day of week	Saturday	Friday	Saturday	Sunday

[a]Slope of a least squares regression. Value in parenthesis is r^2, square of correlation coefficient.
[b]Average value of ratio in plume.

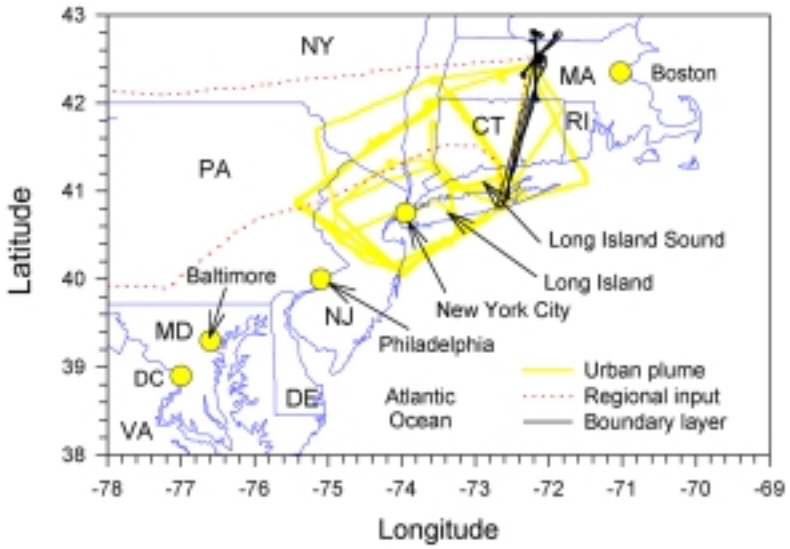

Figure 1. Map of the northeastern United States identifying places referred to in the text. Composite ground track of the DOE G-1 aircraft shows flights grouped by objectives. Test flights are not shown.

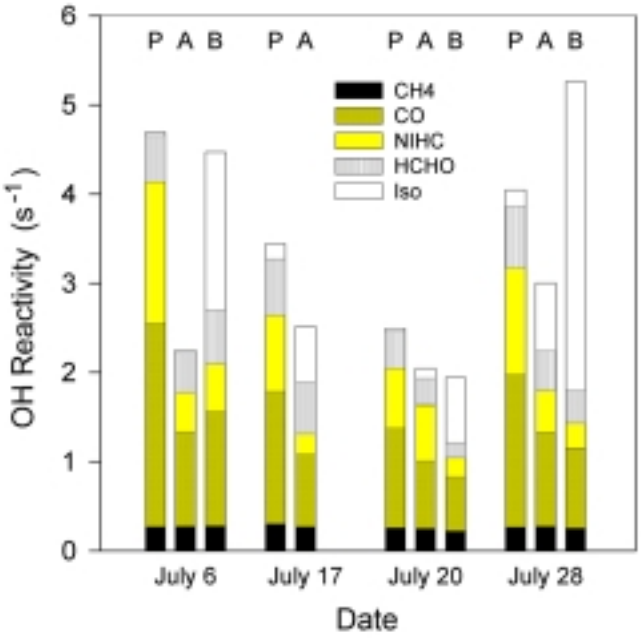

Figure 2. Reactivity of CH_4, CO, non-isoprene hydrocarbons (NIHC), HCHO, and isoprene with respect to OH, as defined by equation (1). Locations are indicated as being from the plume (P), adjacent to the plume (A), or upwind background (B). Locations A and B are the same as those used in Table 1. Plume values of NIHC and Isoprene for July 20 and 28 are from VOC samples taken near the O_3 maximum. There were no in-plume VOC samples for July 6 and July 17. NIHC on these days is determined from the correlation between CO and individual hydrocarbons for the entire data set; isoprene is determined by location. Background reactivities are from one-, two-, and three-sample averages on July 6, 20, and 28, respectively. CH_4 concentration is assumed to be 1700 ppb. Isoprene reactivity contains contributions from methyl vinyl ketone (MVK) and methacrolein (MACR).

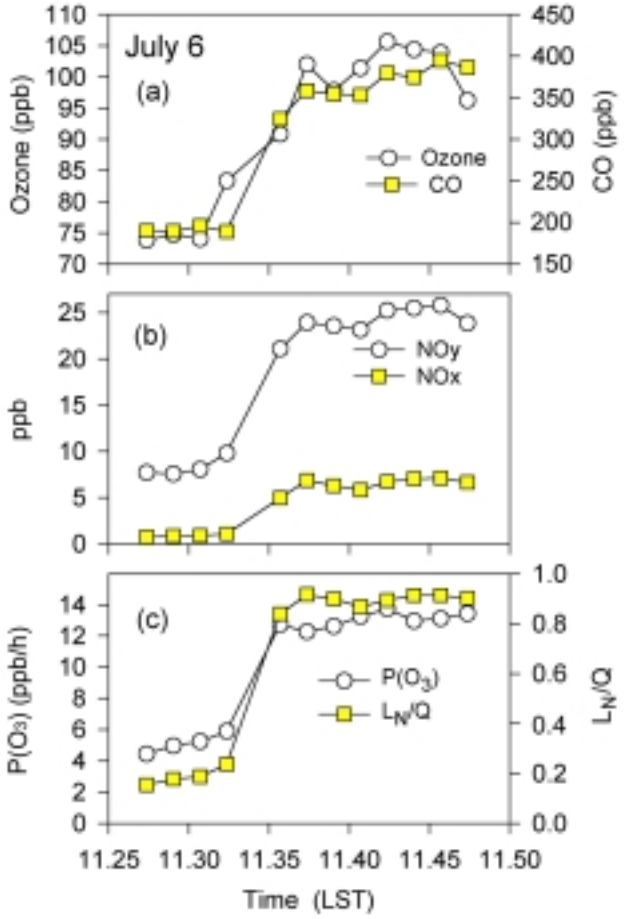

Figure 3. Trace gas concentrations and calculated quantities for the July 6 plume traverse. Geographic location is shown in Plate 2. (top) One minute average observed value of O_3 and CO. (middle) One minute average observed value of NO_y and NO_x. (bottom) Calculated value of O_3 production rate, $P(O_3)$, and the fraction of radicals that are removed by reacting with NO_x, L_N/Q.

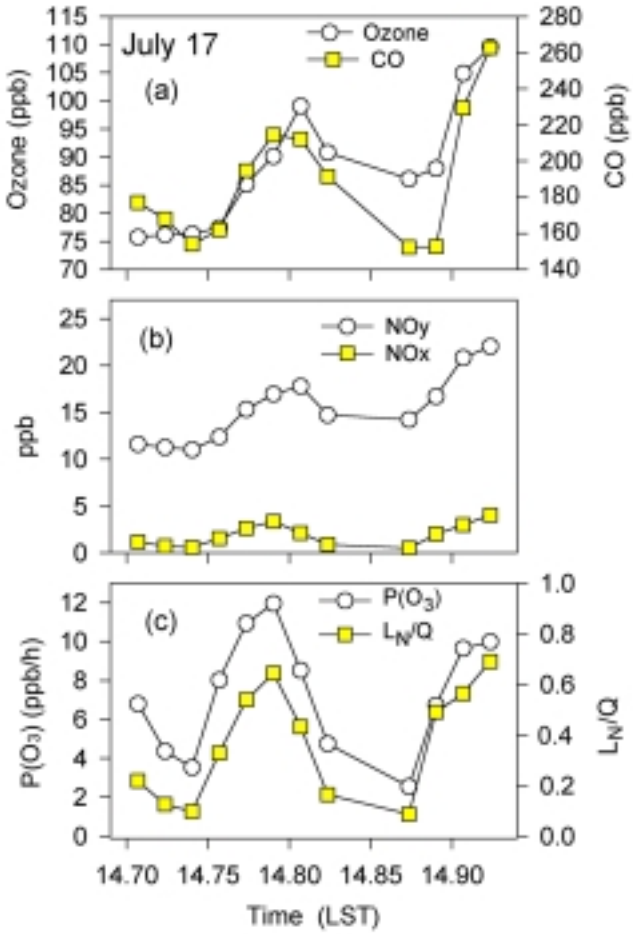

Figure 4. Trace gas concentrations and calculated quantities for the July 17 plume traverse. Geographic location is shown in Plate 2. Same format as Figure 3.

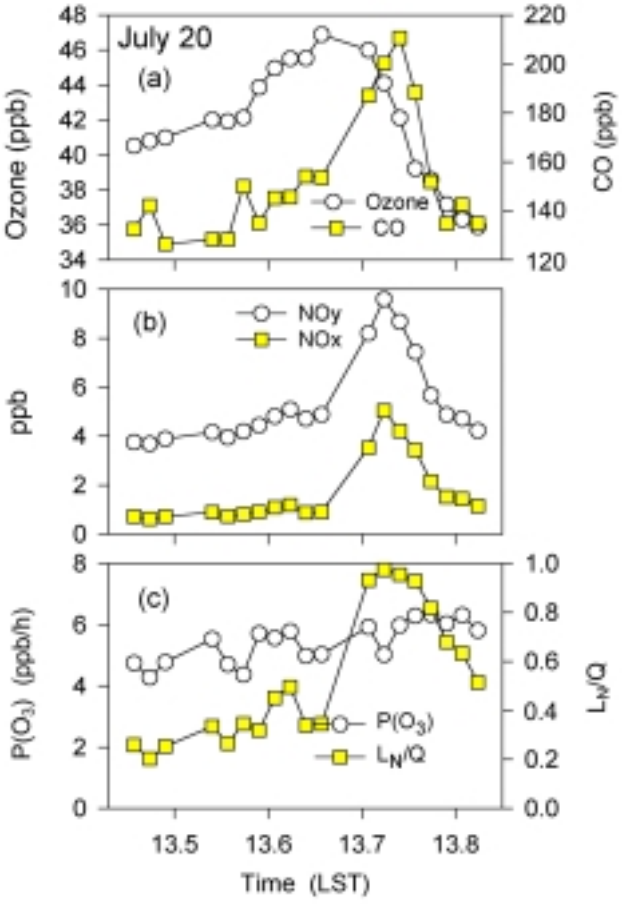

Figure 5. Trace gas concentrations and calculated quantities for the July 20 plume traverse. Geographic location is shown in Plate 2. Same format as Figure 3.

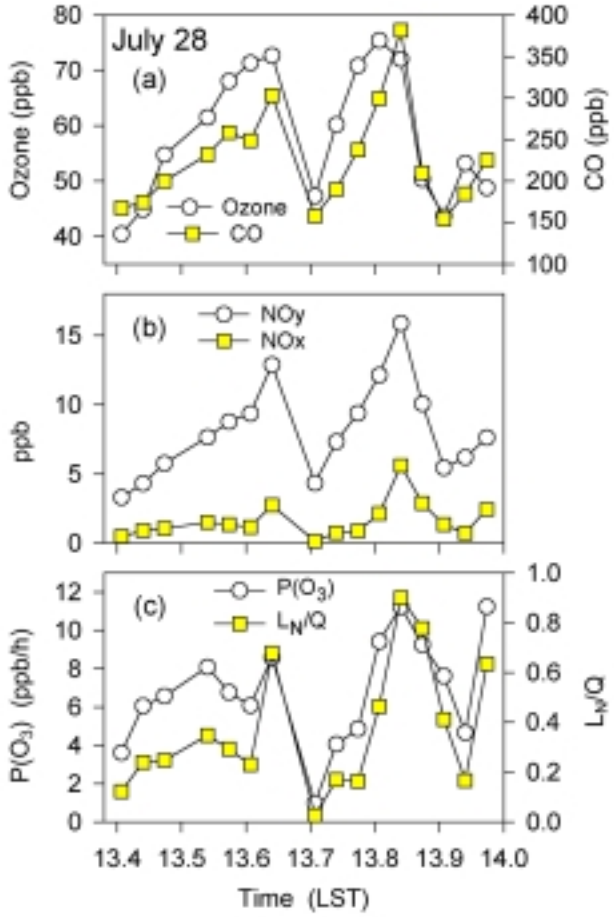

Figure 6. Trace gas concentrations and calculated quantities for the July 28 plume traverse. Geographic location is shown in Plate 2. Same format as Figure 3.

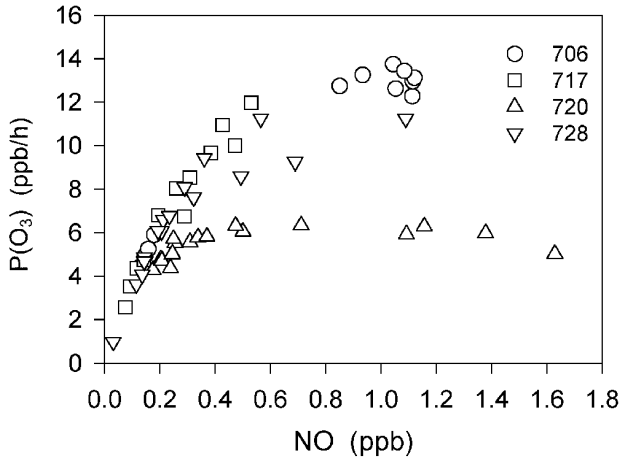

Figure 7. Calculated values of $P(O_3)$ versus observed concentration of NO. Points on graph are from plume and adjacent-to-plume locations depicted in Figures 3-6.

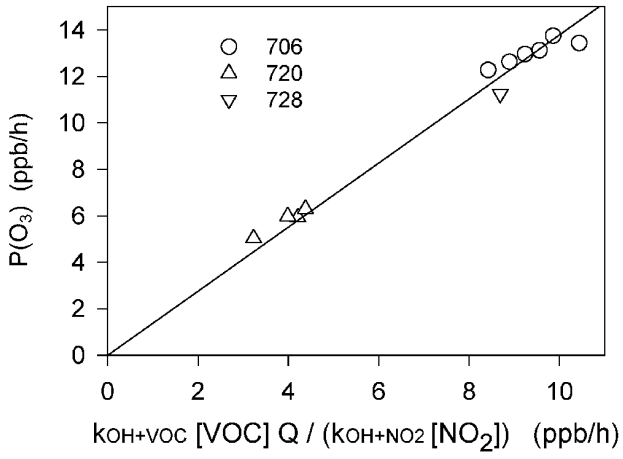

Figure 8. Calculated values of $P(O_3)$ versus $k_1[VOC]Q/(k_2[NO_2])$ as a test of the high-NO_x relation, given by equation (4). Quantities are defined in text. Points on graph are a subset of points from Figure 7, with [NO] >1 ppb. Straight line is a regression fit to data with zero intercept. The slope yields an empirical estimate of the factor Y in equation (4). The slope gives an average of 1.4 O_3 molecules formed per OH + VOC reaction.

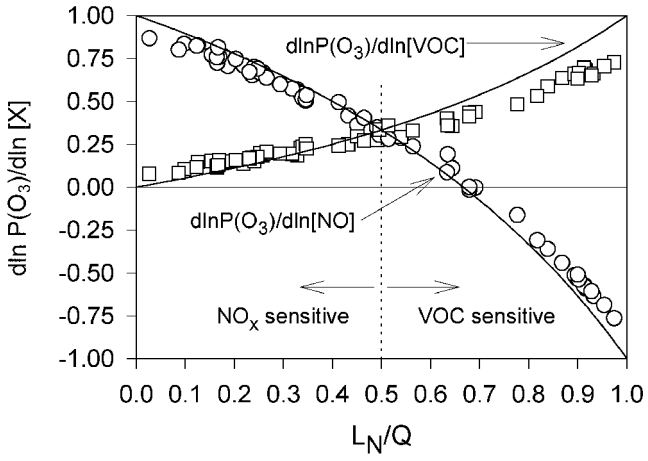

Figure 9. Relative sensitivity of $P(O_3)$ with respect to changes in the concentration of NO or VOCs, $d\ln P(O_3)/d\ln$ [NO] and $d\ln P(O_3)/d\ln$ [VOC], respectively. Points on graph are from plume and adjacent-to-plume locations depicted in Figures 3-6. Curved lines are analytic functions given in equations (6) and (7).

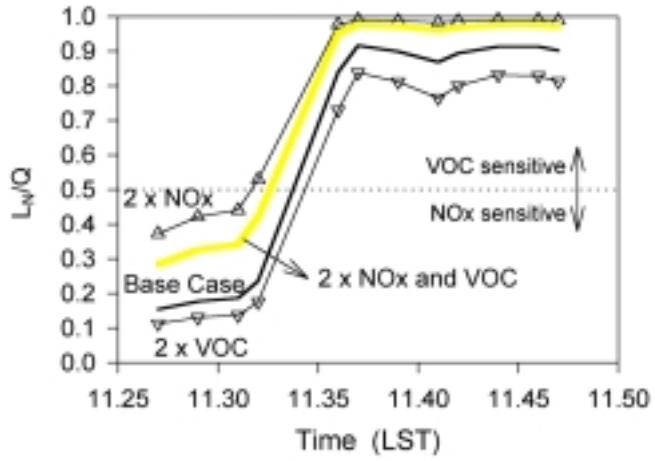

Figure 10. Calculated value of L_N/Q for varied NO_x and VOC concentrations. Base case July 6 data points are the same as those used in Figure 3. Calculations were done with NO_x doubled, VOCs doubled and both doubled.

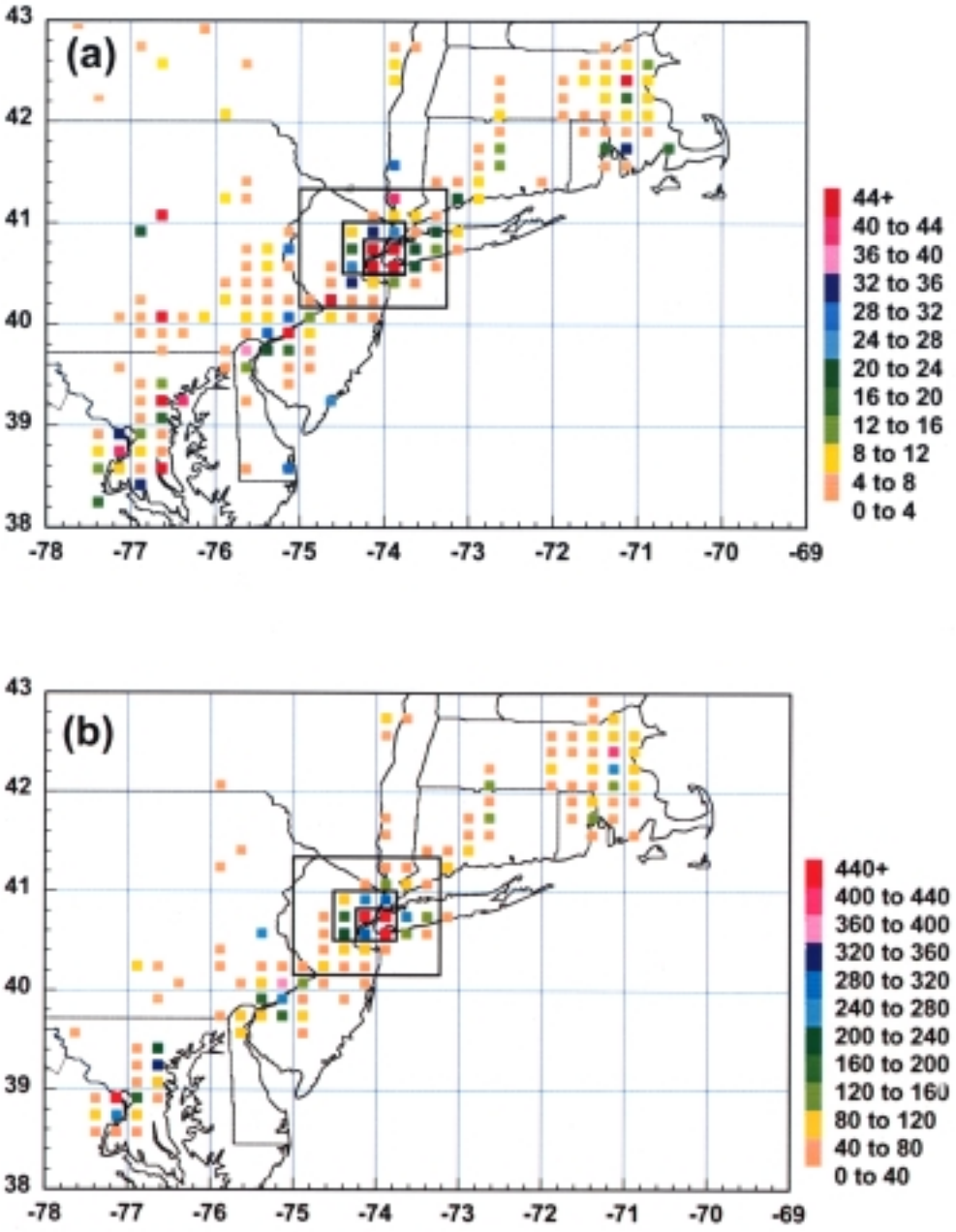

Plate 1. (a) NO_x and (b) CO emission rates in units of 10^{11} molecules cm^{-2} s^{-1} according to the 1990 National Acid Precipitation Assessment Program (NAPAP) inventory. Emission inventories include anthropogenic point, area, and mobile source categories. Spatial resolution is 1/4˚ longitude by 1/6˚ latitude. Emission rates are for a summer weekday. Three boxes centered on New York City are used to specify areas with different emission densities as described in text.

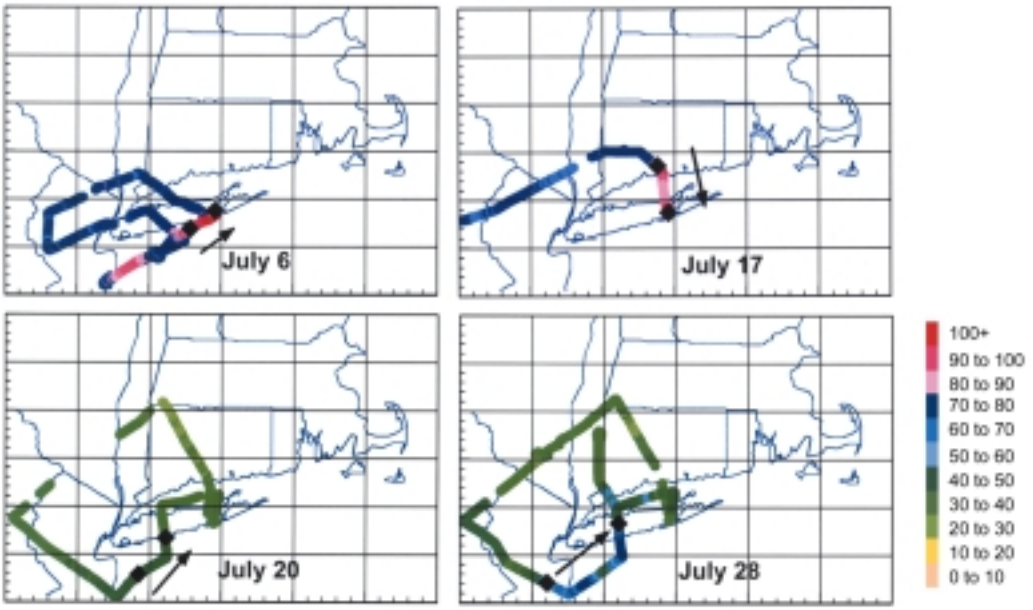

Plate 2. Ground track of the DOE G-1 aircraft on July 6, 17, 20, and 28 color coded to indicate O_3 concentration. Flight segments during instrument zeroes or above 1200 m have been omitted. Plume regions are in between black diamonds. Arrows indicate approximate size of plume and direction of G-1. Flight times (LST) are 0846-1132 on July 6, 1203-1458 on July 17, 1132-1414 on July 20, and 1143-1447 on July 28.

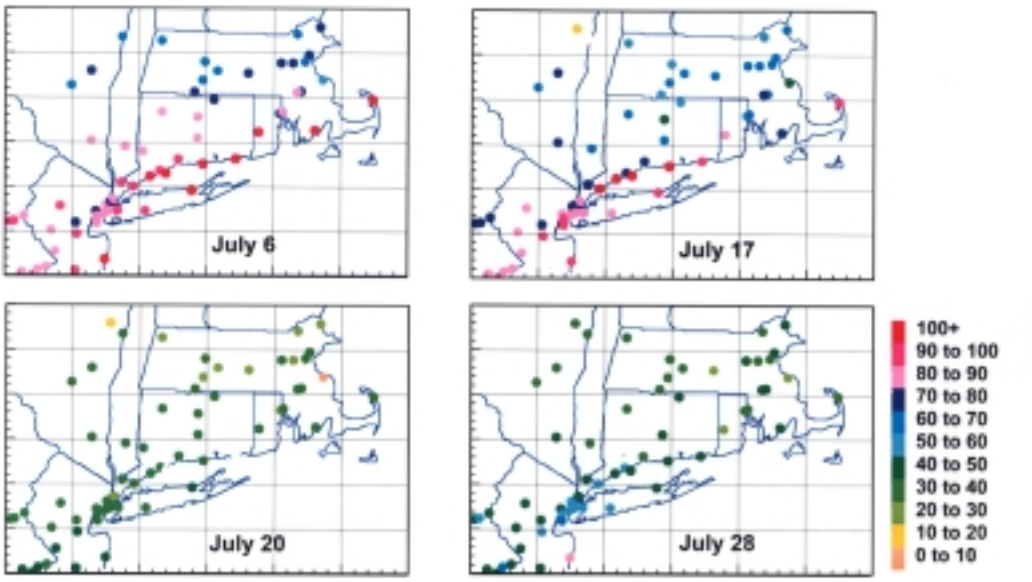

Plate 3. Surface O_3 concentration at 1400 LST as measured by EPA sites within the State/Local Air Monitoring Station SLAMS network [*Roberts et al.*, 1996a]. Dates are indicated on plate. On July 6, maximum O_3 levels of 114-117 ppb were observed at 1400 LST at the eastern Connecticut shore stations. On July 17, maximum O_3 levels of 111-118 ppb occurred between 1400 and 1600 LST at the central and eastern Connecticut shore stations.

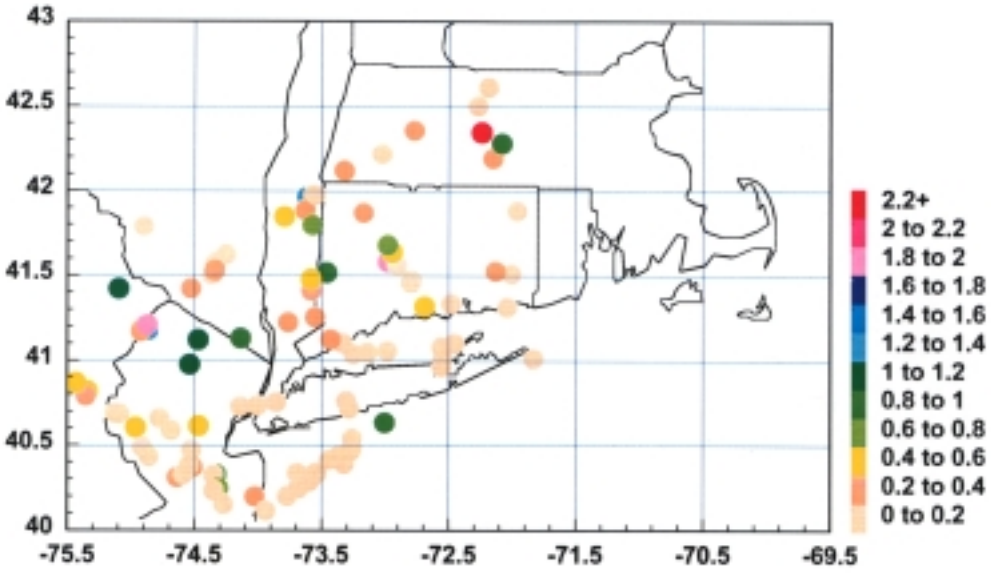

Plate 4. Isoprene concentration in parts per billion. Sample altitude is below 1000 m.